

Article

GECM-Based Voltage Stability Assessment Using Wide-Area Synchrophasors

Heng-Yi Su * and Tzu-Yi Liu

Department of Electrical Engineering, Feng Chia University (FCU), No. 100, Wenhwa Road, Seatwen, Taichung 40724, Taiwan; M0522016@fcu.edu.tw

* Correspondence: hengyisu@fcu.edu.tw; Tel.: +886-4-2451-7250 (ext. 3822)

Received: 21 September 2017; Accepted: 10 October 2017; Published: 13 October 2017

Abstract: Voltage instability is a crucial issue in the secure operation of power grids. Several methods for voltage stability assessment were presented. Some of them are highly computationally intensive, while others are reported not to work properly under all circumstances. This paper proposes a new methodology based on the generator equivalent circuit model (GECM) and the phasor measurement unit (PMU) technology for online voltage stability monitoring of a power grid. First, the proposed methodology utilizes synchronized phasor (synchrophasor) measurements to determine the impedance parameters of a transmission grid by means of the recursive least squares (RLS) algorithm. Furthermore, it incorporates the dynamic models of generators to handle the cases with generator reactive power limit violations. After that, an enhanced voltage stability index with GECMs incorporated is developed for reliable and accurate voltage stability assessment. The proposed methodology was first demonstrated on several standard IEEE power systems, and then applied to a practical power system, the Taiwan power (Taipower) system. The test results demonstrate the flexibility and effectiveness of the proposed methodology.

Keywords: generator equivalent circuit model; online security assessment; phasor measurement unit (PMU); smart grid; voltage collapse; voltage instability; wide-area measurement system (WAMS)

1. Introduction

Voltage instability has become a challenging issue in power grids since several major blackouts worldwide have been mainly attributed to voltage collapse [1–3]. Voltage collapse tends to occur during heavy loading, especially when the generating capacity is insufficient. Indeed, it can also be caused by a contingency, such as the loss of a crucial generator or transmission line, or some of the critical buses in the system not providing adequate reactive power support [4,5].

Since the wide-area measurement system (WAMS) has become a core technology in future smart grids, the ability commended from this technology has been perceived globally with its effective analysis on a variety of applications in power grid monitoring, control, and protection [6,7]. A typical WAMS comprises of phasor measurement units (PMUs), phasor data concentrators (PDCs), control center, and high-speed data communication infrastructures. Over the past years, several countries have installed PMUs to form WAMS on their power systems [8]. PMUs are precise power system measuring devices that provide the information of voltage and current phasors and frequency at a very high speed (usually 30 measurements per second). Measurements from PMUs are then time-stamped according to a high precision common time reference given by global positioning system (GPS). These time-synchronized phasor (synchrophasor) measurements include sufficient information for monitoring voltage stability of a transmission grid [9–12].

To examine the proximity to voltage instability, a variety of approaches were presented, such as singular value decomposition [13], continuation power flow [14,15], and Thevenin equivalent (TE)

model [16–24]. Many of these studies have developed voltage stability indices, which aims to show how far the system is away from a possible instability event. In [18], for example, a local voltage stability index using single-port TE model to estimate voltage stability margin was developed. To enhance the performance of single-port TE, several voltage stability indices based on coupled single-port TE were presented in [19–24], where the work [24] develops a L-index for system voltage stability analysis. The L-index is well suited for online applications. However, the original L-index fails to perform as expected in some cases [25]. In addition, an accurate system model is required for this kind of index. Nevertheless, model parameters and the transmission network topology usually vary with time. In other words, it is difficult to obtain a correct modeling. Without correct transmission grid modeling, the performance of this index would be degraded.

In this context, the main contribution of this study is to develop a novel online voltage stability monitoring approach for secure and reliable grid operations. To this aim, a new voltage stability indicator based on the GECM and the PMU technique is proposed. With the utilization of PMU measured data in real-time, wide-area voltage stability situational awareness for system operators can be enhanced. Moreover, the proposed approach is able to handle the cases with generator Q limits violation.

In this paper, a brief description of the synchrophasor technique and the basic concept of the L-index for voltage stability assessment are provided in Section 2. Section 3 describes the GECM and the synchrophasor technique used to track changing parameters of transmission grid impedance models, considering the dynamic behavior of system generators. After that, an enhanced voltage stability index with GECMs incorporated is thoroughly described. The capability of utilizing the presented methodology in voltage stability assessment is verified in Section 4, followed by the conclusions given in Section 5.

2. Preliminaries

2.1. Synchrophasor Technique

With the advent of WAMS, there is a trend toward utilizing wide-area synchrophasor data in transmission grid monitoring, control, and protection. A complete explanation of the synchrophasor technique can be found in [6]; however, its main points are given here.

Synchrophasors are precise measurements provided by a PMU, which is available as a standalone physical device or functional device within another unit. A single PMU, when deployed at a bus, can directly capture the voltage phasor at bus and the current phasors on the incident lines. For example, suppose that a PMU is deployed at bus i , as shown in Figure 1. Thus, the voltage phasor $V_i = |V_i| \angle \theta_i$ at bus i and the current phasors $I_{ij} = |I_{ij}| \angle \theta_{ij}$ and $I_{ik} = |I_{ik}| \angle \theta_{ik}$ through the lines connected to bus j and bus k can be measured in real-time using the installed PMU.

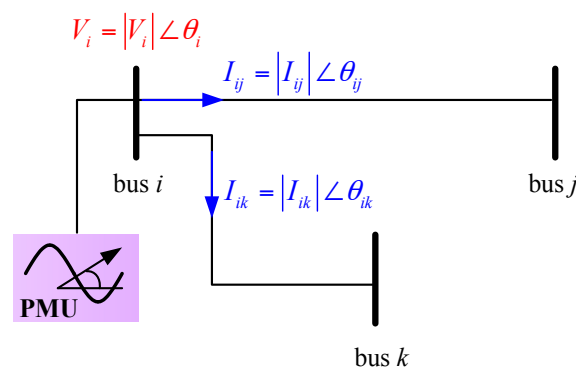


Figure 1. Three-bus system with phasor measurement unit (PMU) installed at bus i .

Indeed, having the accurate synchrophasor measurements, the control center is able to gather high resolution phase information that allows for operators to initiate immediate proper response within seconds and this may lead to much more highly secured power system network from blackout events [7]. In addition, the deliberate revolution by employing WAMS in power systems has boosted the performance in monitoring, analysis, and control functions.

2.2. Original L-Index

One of the most popular indicators for voltage stability analysis is the L-index. It was originally presented in the work [24]. This method is referred as the *reference method* in this research.

Let $(\mathbf{V}_L, \mathbf{I}_L)$ and $(\mathbf{V}_G, \mathbf{I}_G)$ be the voltages and currents at load and generator buses, respectively. Given the system admittance matrix Y , the relationship between bus voltages and currents is

$$\begin{bmatrix} \mathbf{I}_G \\ \mathbf{I}_L \end{bmatrix} = \begin{bmatrix} Y_{GG} & Y_{GL} \\ Y_{LG} & Y_{LL} \end{bmatrix} \begin{bmatrix} \mathbf{V}_G \\ \mathbf{V}_L \end{bmatrix} \quad (1)$$

where Y_{GG} , Y_{GL} , Y_{LG} and Y_{LL} are submatrices of Y corresponding to generator and load buses. Rearranging (1) gives

$$\begin{bmatrix} \mathbf{V}_L \\ \mathbf{I}_G \end{bmatrix} = \begin{bmatrix} Z_{LL} & K \\ Y_{GG}Z_{LL} & Y_{GG} + Y_{GL}K \end{bmatrix} \begin{bmatrix} \mathbf{I}_L \\ \mathbf{V}_G \end{bmatrix} \quad (2)$$

where $Z_{LL} = Y_{LL}^{-1}$ and $K = -Y_{LL}^{-1}Y_{LG}$.

For any load bus $i \in \alpha_L$, where α_L denotes a set of load buses, the index L_i is defined as [24]

$$L_i = \left| 1 - \frac{[KV_G]_j}{V_{Li}} \right|, \quad i \in \alpha_L, \quad j \in \alpha_G \quad (3)$$

where α_G denotes a set of generator buses. The L-index theoretically varies from 0 at no load to 1 at voltage collapse. However, this is not always true for all the cases [25]. In some cases, the value of the system L-index at voltage-collapse point is much less than the supposed theoretical limit of 1, whereas in some cases the value of the system L-index at voltage-collapse point is much greater than 1. In other words, the original L-index may not be utilized as an absolute indicator in voltage stability analysis.

In addition, a drawback of the L-index is that it assumes a constant V_G during load increase. When Q limits are encountered at the generator buses, this will no longer be the case. On the other hand, an accurate system model is required for the L-index in computing the matrix $K = -Y_{LL}^{-1}Y_{LG}$ used in Equation (3). However, a correct modeling is hard to be acquired due to the fact that model parameters and the transmission network topology usually vary with time. To address these difficulties, a new voltage stability indicator based on the GECM and the PMU technique is presented in this research.

3. Proposed Methodology

In this research, a WAMS-based method to online voltage stability monitoring is presented. It was designed to cope with the cases of generator Q limits violated. This justifies its use for practical voltage stability analysis.

The overall diagram of the proposed method is shown in Figure 2, in which the proposed method is demonstrated with the section surrounded by a dashed line. Indeed, the proposed method consists of three stages in computational procedures. The first stage aims at determining the GECMs using generator parameters and PMU data. At the second stage, the RLS algorithm with PMU data are employed to estimate the single-branch TE circuits with GECMs. Then, the enhanced voltage stability index with GECMs can be obtained. Details of the proposed method are described as follows.

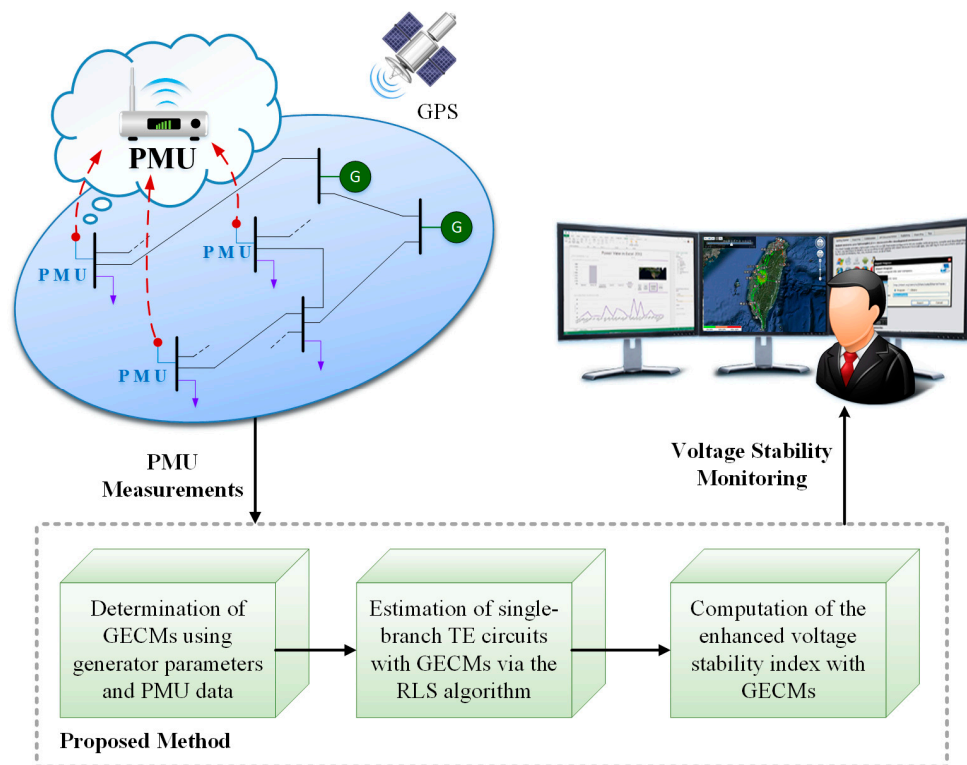


Figure 2. Overview of the proposed methodology.

3.1. Generator Equivalent Circuit Model

In order to deal with generator Q limits violation cases, the GECEM is employed in this study. When considering generator dynamic behaviors, it is assumed that a synchronous generator can be modeled by an internal voltage E_G in series with a generator equivalent impedance Z_G , as shown in Figure 3, in which V_G and I_G are terminal voltage phasor and current phasor of the generator, respectively.

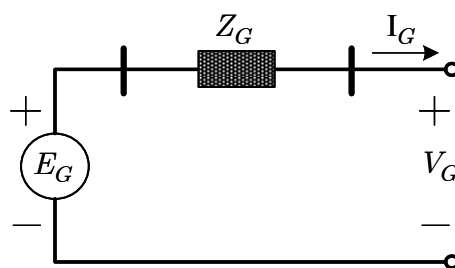


Figure 3. Generator equivalent circuit model (GECEM).

In Figure 3, applying Kirchoff’s voltage law (KVL) to the network yields

$$E_G = V_G + I_G \cdot Z_G \tag{4}$$

Given the generator parameters and direct current and quadrature current, Z_G can be acquired [26,27]. For instance, the 4th-order generator internal impedance Z_G is modeled by

$$Z_G = \frac{[(r_a i_d - (x'_q - x_l) i_q) + j(r_a i_q - (x'_d - x_l) i_d)]}{i_d + j i_q} \tag{5}$$

where

r_a armature resistance;
 x_l leakage reactance;
 x'_q q -axis transient reactance;
 x'_d d -axis transient reactance;
 i_d d -axis current;
 i_q q -axis current.

Suppose that generator parameters (r_a, x_l, x'_q, x'_d) are known and V_G and I_G are acquired from PMUs, time-varying parameters E_G and Z_G can be estimated, i.e., the GECMs can be obtained.

3.2. Transmission Grid Modeling with GECMs

A general transmission grid model is illustrated in Figure 4. Suppose that such grid model is composed of k generators and n loads. When considering the dynamic behavior of system generators, the GECM, which is able to track generator dynamic behaviors, is utilized. That is, k generators in this study are modeled by their GECMs with time-varying E_G and Z_G . It is noteworthy that the GECM is adequate for both PV generators and PQ generators [26,27].

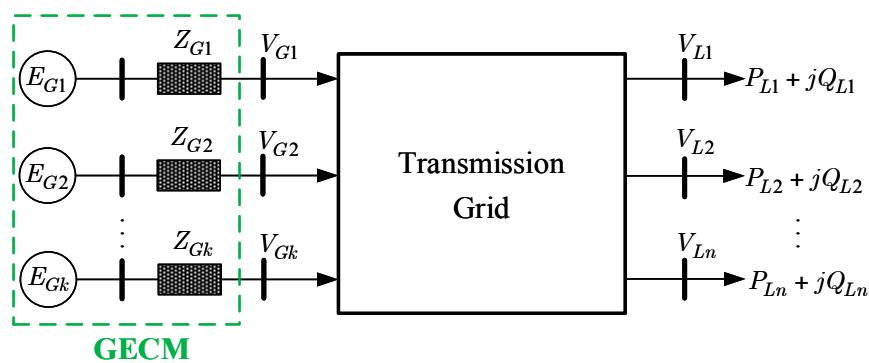


Figure 4. Multi-node network transmission grid model where generators are modeled by the GECMs.

Indeed, the network shown in Figure 4 can be modeled by a multi-branch TE circuit. Let \mathbf{I}_{GECM} be the vector of bus currents and \mathbf{V}_{GECM} be the vector of bus voltages. The node-voltage equation, which includes the internal nodes of the machines, is written as

$$\mathbf{I}_{GECM} = Y_{GECM} \mathbf{V}_{GECM} \quad (6)$$

where $\mathbf{I}_{GECM} = [\mathbf{I}_G \quad \mathbf{I}_L \quad \mathbf{0}]^T$ and $\mathbf{V}_{GECM} = [\mathbf{E}_G \quad \mathbf{V}_L \quad \mathbf{V}_G]^T$; Y_{GECM} is the system admittance matrix with generator equivalent admittance denoted by $Y_{gg} = \text{diag}(1/Z_{G_i} | i = 1, 2, \dots, k)$; and, the subscripts G and L denote generator buses and load buses, respectively. In Equation (6), \mathbf{V}_L can be expressed by

$$\mathbf{V}_L = K_{GECM} \mathbf{E}_G + Z_{GECM} \mathbf{I}_L \quad (7)$$

where $K_{GECM} \in \mathbb{R}^{k \times n}$ and $Z_{GECM} \in \mathbb{R}^{n \times n}$ denote the transmission grid voltage gain matrix and impedance matrix, respectively. In this work, an approach based on synchrophasors is presented to estimate K_{GECM} and Z_{GECM} .

3.3. Online Estimation of Transmission Grid Model with GECMs

With increasing deployment of PMUs across transmission grids, wide are the measurements that can be obtained from WAMS. In order to make the transmission grid be fully observable,

suppose that PMUs are deployed optimally by means of the approach presented in [8]. In this case, time-synchronized (V_L, I_L) and (V_G, I_G) are available. Also, E_G of GECM can be estimated from PMU measured data via Equation (4).

Suppose that there are t measurements obtained from PMUs, Equation (7) can be expressed as

$$\mathbf{V}_L^i = K_{GECM} \mathbf{E}_G^i + Z_{GECM} \mathbf{I}_L^i \quad (8)$$

for each $i = 1, 2, \dots, t$. The above equation is further rearranged as

$$Y_t = \theta H_t \quad (9)$$

where

$$Y_t = \begin{bmatrix} \mathbf{V}_L^1 & \mathbf{V}_L^2 & \dots & \mathbf{V}_L^t \end{bmatrix} \quad (10)$$

$$H_t = \begin{bmatrix} \mathbf{E}_G^1 & \mathbf{E}_G^2 & \dots & \mathbf{E}_G^t \\ \mathbf{I}_L^1 & \mathbf{I}_L^2 & \dots & \mathbf{I}_L^t \end{bmatrix} \quad (11)$$

$$\theta = \begin{bmatrix} K_{GECM} & Z_{GECM} \end{bmatrix} \quad (12)$$

The least-square estimate of the parameters θ in Equation (9) is

$$\hat{\theta} = Y_t H_t^* (H_t H_t^*)^{-1} \quad (13)$$

In our application, the data from PMU is coming in sequentially, which means that the size of H_t will be increased if a new data point is available. This can also result in computational complexity for the estimation of θ via Equation (13). Due to memory and computational issues, the traditional least-square method is not suitable for on-line applications.

In this study, the recursive least square (RLS) algorithm, which combines the old estimate and the new data, is applied to solve the unknown θ in Equation (9) iteratively. First, define P_t^{-1} as $H_t H_t^*$, such that

$$\begin{aligned} P_t^{-1} &= H_t H_t^* \\ &= P_{t-1}^{-1} + \mathbf{h}_t \mathbf{h}_t^* \end{aligned} \quad (14)$$

where $\mathbf{h}_t = \begin{bmatrix} \mathbf{E}_G^t & \mathbf{I}_L^t \end{bmatrix}^T$. Also, the term $Y_t H_t^*$ in Equation (13) can be written as

$$Y_t H_t^* = Y_{t-1} H_{t-1}^* + \mathbf{V}_L^t \mathbf{h}_t^* \quad (15)$$

Substituting Equations (14) and (15) into Equation (13) gives

$$\begin{aligned} \hat{\theta}_t &= Y_t H_t^* P_t \\ &= (Y_{t-1} H_{t-1}^* + \mathbf{V}_L^t \mathbf{h}_t^*) P_t \end{aligned} \quad (16)$$

Since $\hat{\theta}_{t-1} = Y_{t-1} H_{t-1}^* P_{t-1}$, then

$$\hat{\theta}_{t-1} P_{t-1}^{-1} = Y_{t-1} H_{t-1}^* \quad (17)$$

Substituting for $Y_{t-1} H_{t-1}^*$ in Equation (16) gives

$$\hat{\theta}_t = (\hat{\theta}_{t-1} P_{t-1}^{-1} + \mathbf{V}_L^t \mathbf{h}_t^*) P_t \quad (18)$$

Rearrange Equation (14) as $P_{t-1}^{-1} = P_t^{-1} - \mathbf{h}_t \mathbf{h}_t^*$. Substituting for P_{t-1}^{-1} into Equation (18) and rewriting this equation, yields

$$\begin{aligned}\hat{\theta}_t &= (\hat{\theta}_{t-1} P_{t-1}^{-1} - \hat{\theta}_{t-1} \mathbf{h}_t \mathbf{h}_t^* + \mathbf{V}_L^t \mathbf{h}_t^*) P_t \\ &= \hat{\theta}_{t-1} + (\mathbf{V}_L^t - \hat{\theta}_{t-1} \mathbf{h}_t) \mathbf{h}_t^* P_t\end{aligned}\quad (19)$$

From Equation (14), we conclude that $P_t = (P_{t-1}^{-1} + \mathbf{h}_t \mathbf{h}_t^*)^{-1}$. Substituting for P_t in Equation (19) and using the matrix inversion lemma, we get

$$\begin{aligned}\hat{\theta}_t &= \hat{\theta}_{t-1} + (\mathbf{V}_L^t - \hat{\theta}_{t-1} \mathbf{h}_t) \mathbf{h}_t^* P_t \\ \mathbf{K}_t &= P_{t-1} \mathbf{h}_t (1 + \mathbf{h}_t^* P_{t-1} \mathbf{h}_t)^{-1} \\ P_t &= (I - \mathbf{K}_t \mathbf{h}_t^*) P_{t-1}\end{aligned}\quad (20)$$

where I is the identity matrix. In order to track time-varying parameters, the forgetting factor approach is used to modify Equation (20). The modified RLS algorithm with the forgetting factor ψ becomes

$$\begin{aligned}\hat{\theta}_t &= \hat{\theta}_{t-1} + (\mathbf{V}_L^t - \hat{\theta}_{t-1} \mathbf{h}_t) \mathbf{h}_t^* P_t \\ \mathbf{K}_t &= P_{t-1} \mathbf{h}_t (\psi + \mathbf{h}_t^* P_{t-1} \mathbf{h}_t)^{-1} \\ P_t &= [(I - \mathbf{K}_t \mathbf{h}_t^*) P_{t-1}] / \psi\end{aligned}\quad (21)$$

Note that the smaller the value of ψ , the quicker information obtained from previous data will be forgotten.

3.4. Enhanced Voltage Stability Index

In order to handle generator reactive power limits violation cases, a new index L^{new} with GECMs incorporated is described here.

Using the method presented in Section 3.3, single-branch TE circuits with GECMs can be estimated by using PMU data. That is the matrix K_{GECM} , which includes the effects of generator reactive-power limits, is acquired. In addition, instead of using constant \mathbf{V}_G as Equation (3) for original L-index, the time-varying \mathbf{E}_G of GECMs is utilized. Thus, the enhanced index L^{new} for a load bus i is given by

$$L_i^{new} = \left| 1 - \frac{[K_{GECM} \mathbf{E}_G]_j}{V_{Li}} \right|, \quad i \in \alpha_L, \quad j \in \alpha_G \quad (22)$$

Note that the range of L_i^{new} is $[0, 1]$. When voltage collapse occurs, $L_i^{new} = 1$. Thus, the overall system index can be expressed as

$$L_{\max}^{new} = \max_{i \in \alpha_L} \{L_i^{new}\} \quad (23)$$

The main steps of the proposed PMU-based algorithm to voltage stability assessment are presented in Algorithm 1.

In Algorithm 1, the proposed method uses the given generator parameters and the measured PMU data to determine time-varying \mathbf{E}_G and \mathbf{Z}_G of GECMs (steps 2 to 5). The transmission grid model $\theta = \begin{bmatrix} K_{GECM} & Z_{GECM} \end{bmatrix}$ with GECMs is estimated by means of the RLS algorithm (step 6). K_{GECM} is then obtained (step 7). For each load bus i , L_i^{new} is calculated by using the estimated K_{GECM} and the computed \mathbf{E}_G (steps 8 to 10). After that, find the maximum value of L_i^{new} which is utilized to represent the voltage stability index of the entire system (step 11).

Algorithm 1 Proposed PMU-Based Algorithm to Voltage Stability Assessment.

```

1: Input:  $(r_a, x_l, x'_q, x'_d), (V_L, I_L),$  and  $(V_G, I_G);$ 
2: for  $j \in \alpha_G$  do
3:   Compute  $Z_{Gj}$  by Equation (5);
4:   Compute  $E_{Gj}$  by Equation (4);
5: end for
6: Estimate  $\theta = \begin{bmatrix} K_{GECM} & Z_{GECM} \end{bmatrix}$  using the RLS algorithm;
7:  $K_{GECM} \leftarrow$  submatrix of  $\theta = \begin{bmatrix} K_{GECM} & Z_{GECM} \end{bmatrix};$ 
8: for  $i \in \alpha_L$  do
9:   Compute  $L_i^{new}$  by Equation (22);
10: end for
11:  $L_{max}^{new} \leftarrow \max_{i \in \alpha_L} \{L_i^{new}\};$ 
12: return  $L_{max}^{new}$ 

```

4. Simulation Results

The proposed methodology in voltage stability assessment has been tested on several IEEE power networks and the Taipower system. For all of the examples, the generators are modeled by their GECMs. The GECM used in this study is the IV order synchronous generator model.

To test the performance of the presented approach for voltage stability assessment, a lot of experiments have been studied. In this research, the following scenarios are considered.

- Load Type: PQ load model and ZIP (constant impedance, current and power) load model
- Load Change Pattern: Single load change, several load change, and all load change
- Generator Q Limits: With and without consideration of generator Q limits

All the test examples were built by the software package of Power System Analysis Toolbox (PSAT) [28], and PSAT is used for running the simulations.

4.1. Case Studies without Generator Q Limits Violation

The IEEE 14 and 118-bus power networks are adopted to illustrate the performance of both the reference method (RM) [24] and the proposed one. System data for the test systems can be found in [29]. The simulations have been carried out to examine the voltage stability index on the test networks. In this case study, all of the loads are increased simultaneously until system loses voltage stability. Also, suppose that there is no generator Q limits violation when the load is increased.

The first test system is the IEEE 14-bus network. Figure 5 shows the L indices at some load levels for this test system, where the figure on the top shows the results obtained by the RM, while the figure on the bottom illustrates the results obtained by the proposed method. From the figure, one can see that bus 14 in this system has the highest index score for the selected load levels. In other words, bus 14 is the most vulnerable bus of the system; therefore, the L-index at bus 14 is selected to be the system L-index.

Figure 6 illustrates the system L-index curves, as well as the continuation curve of bus 14 during the load increase. In this figure, it apparently indicates that the enhanced L-index provided by the proposed method almost reaches the presumed limit of 1 at the voltage collapse point. However, the original L-index provided by the RM fails to do so.

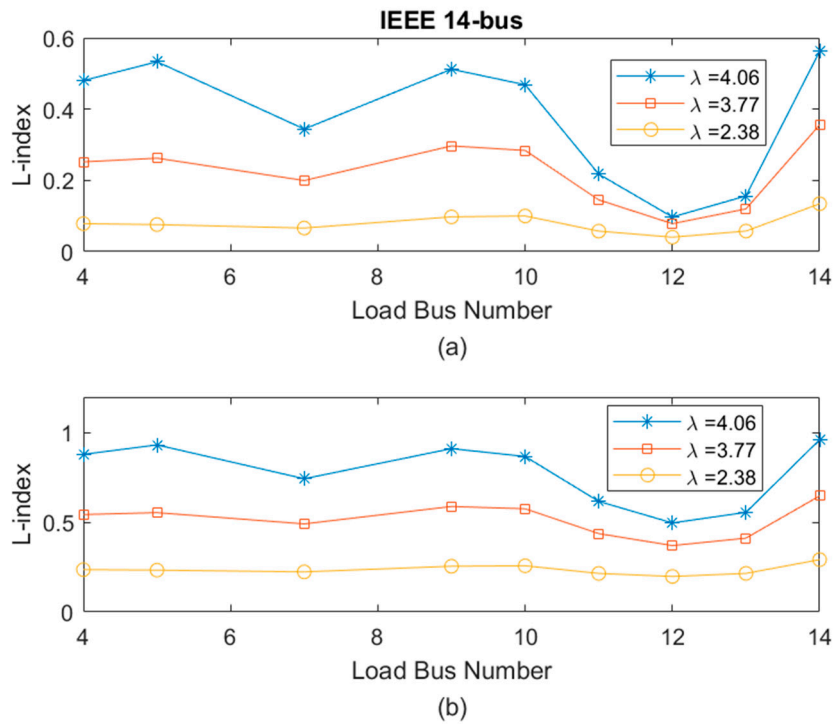


Figure 5. L indices at some load levels for IEEE 14-bus network. (a) Results for the RM; (b) Results for the proposed method.

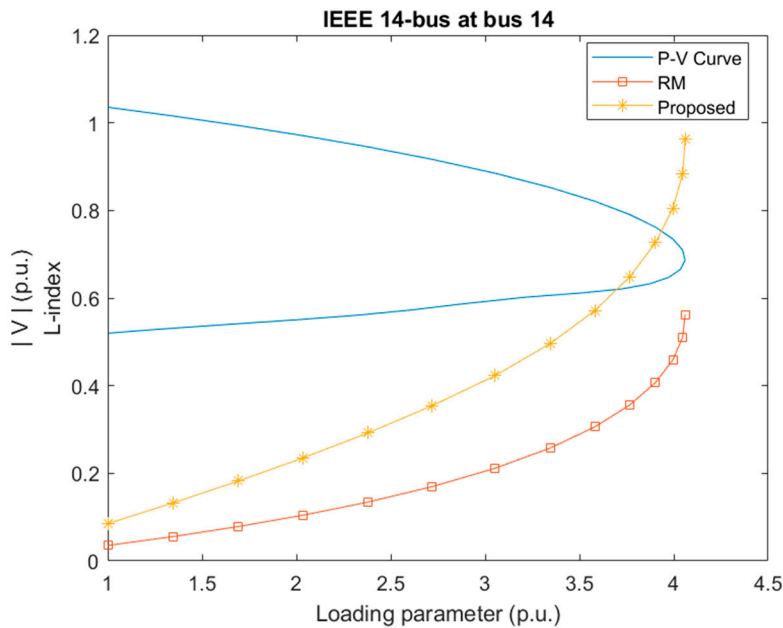


Figure 6. Comparison with L-index between the proposed method and the reference method (RM) at load bus 14 for IEEE 14-bus network.

The second test system is the IEEE 118-bus network. The values of L indices of all the load buses at some selected load levels for the studied system are illustrated in Figure 7, showing that bus 44, which has the maximum value for each load level, is identified as the weakest bus by the RM and the proposed method. Thus, the L-index of bus 44 is chosen as the overall system index.

The results of the L-index at bus 44 for each load level is shown in Figure 8. It indicates that the proposed method achieves the value of 1 at the voltage collapse point, whereas the RM method falls

behind at 0.4835 for the same point. From Figures 6 and 8, it is proven that proposed method can be successfully employed in voltage stability assessment.

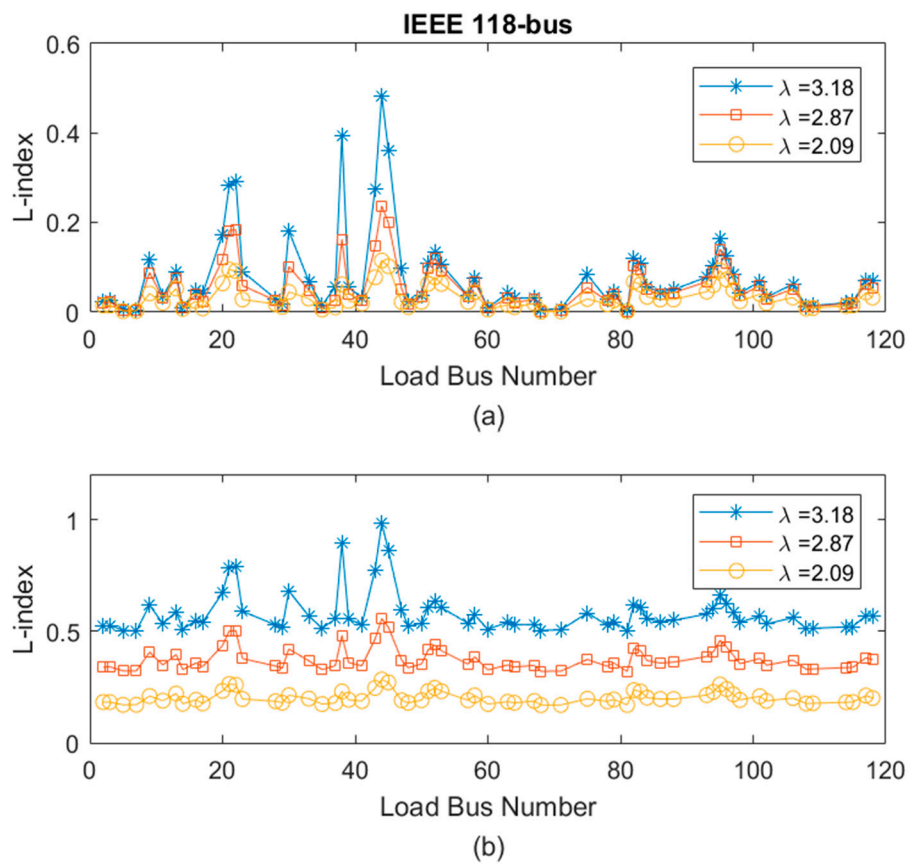


Figure 7. L indices at some load levels for IEEE 118-bus network. (a) Results for the RM; (b) Results for the proposed method.

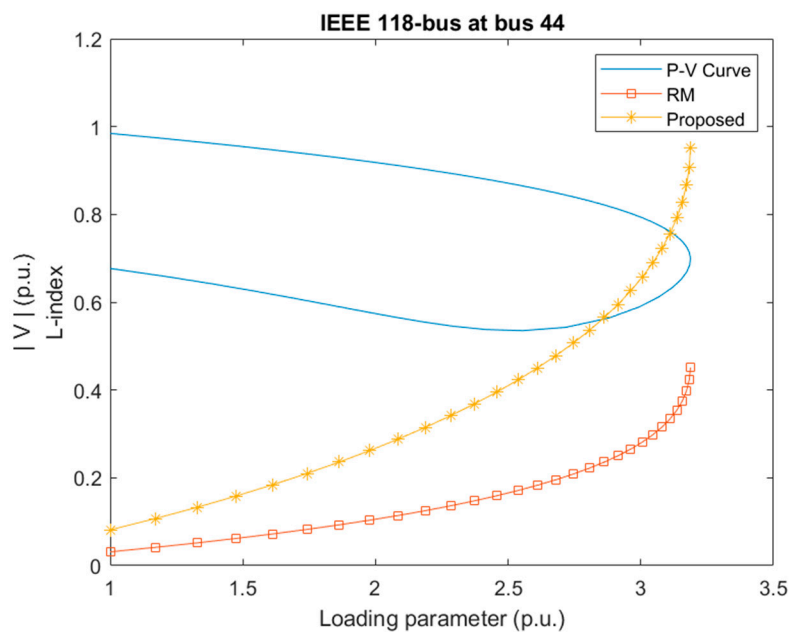


Figure 8. Comparison with L-index between the proposed method and the RM at load bus 44 for IEEE 118-bus network.

4.2. Case Studies with Generator Q Limits Violation

To verify the effect of generator Q limits on voltage stability assessment, many cases have been studied, including different test systems, different initial load levels, different load increase directions, and different Q limit violations. Table 1 lists some selected cases from those investigated cases.

Table 1. Selected cases for the studied system.

Case	Initial Load Level	Load Pattern	Load Variation	Q Limit ¹
1	$\lambda_0 = 0.4$	Single	10%	$\{Q_{Gi}^{Odd} i = 1, 3, 5, \dots\}$
2	$\lambda_0 = 0.8$	Single	10%	$\{Q_{Gi}^{Odd} i = 1, 3, 5, \dots\}$
3	$\lambda_0 = 1.2$	Single	10%	$\{Q_{Gi}^{Odd} i = 1, 3, 5, \dots\}$
4	$\lambda_0 = 0.4$	Several	20%	$\{Q_{Gi}^{Even} i = 2, 4, 6, \dots\}$
5	$\lambda_0 = 0.8$	Several	20%	$\{Q_{Gi}^{Even} i = 2, 4, 6, \dots\}$
6	$\lambda_0 = 1.2$	Several	20%	$\{Q_{Gi}^{Even} i = 2, 4, 6, \dots\}$
7	$\lambda_0 = 0.4$	All	30%	$\{Q_{Gi}^{All} i = 1, 2, \dots, k\}$
8	$\lambda_0 = 0.8$	All	30%	$\{Q_{Gi}^{All} i = 1, 2, \dots, k\}$
9	$\lambda_0 = 1.2$	All	30%	$\{Q_{Gi}^{All} i = 1, 2, \dots, k\}$

Q Limit¹: $\{Q_{Gi}^{Odd} | i = 1, 3, 5, \dots\}$, $\{Q_{Gi}^{Even} | i = 2, 4, 6, \dots\}$ and $\{Q_{Gi}^{All} | i = 1, 2, \dots, k\}$ represent generator reactive power limits at odd generator buses, at even generator buses, and at all generator buses, respectively.

The comparisons with the selected test cases for IEEE 14-bus network are illustrated in Figure 9, where the values of L_{max} corresponding to the test cases (on the x-axis) are depicted on the y-axis of the figure. Due to the effects of generator Q limits violation, the values of L_{max} calculated by the RM are much lower than the critical value of 1. On the contrary, the results given by the proposed approach, which considers the GECMs, are very close to 1. That is, the proposed approach is able to determine the point of voltage collapse even under Q limits violation cases.

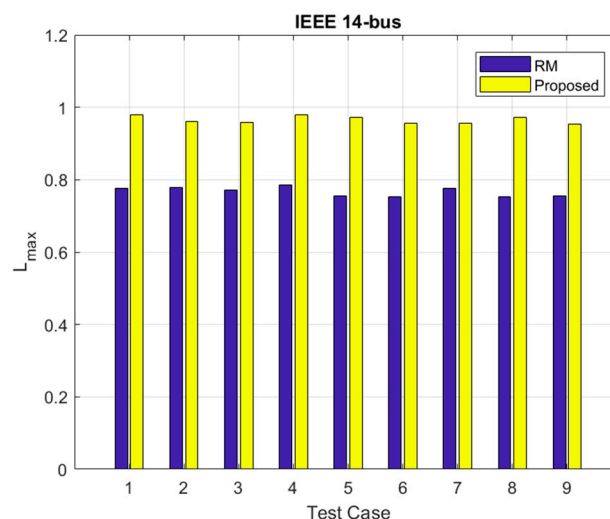


Figure 9. Comparisons for system load at voltage collapse point under different test cases in IEEE 14-bus model. A higher L_{max} indicates a better performance.

Figure 10 demonstrates the results for IEEE 118-bus network. When comparing the results in terms of L_{max} at voltage collapse point for each test case in Figure 10, it indicates that the presented approach performs better than that of the RM, benefiting from the GECMs incorporated. In other words, the presented approach is more suitable to be applied to practical voltage stability assessment with consideration of generator Q limits.

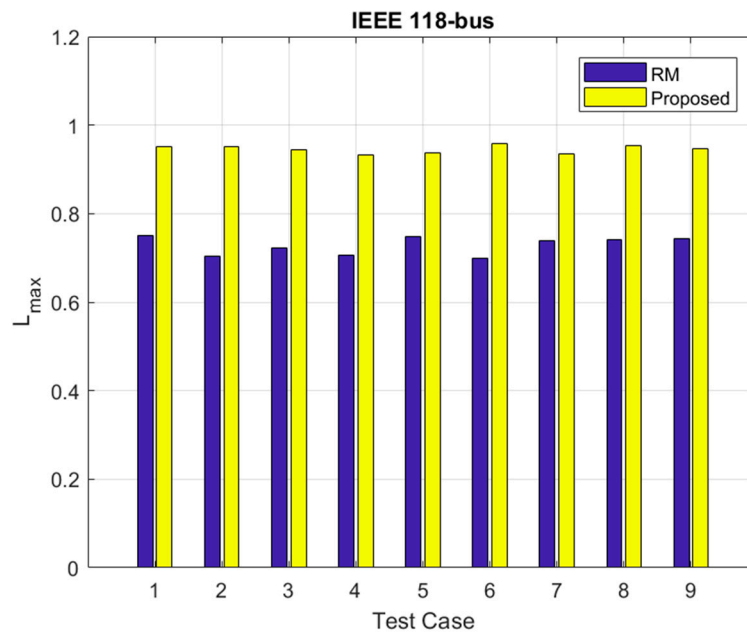


Figure 10. Comparisons for system load at voltage collapse point under different test cases in IEEE 118-bus model. A higher L_{max} indicates a better performance.

4.3. Application to a Practical Power System

The proposed approach has been tested on an actual power system, the Taiwan Power (Taipower) system, composed of 1821 buses, 271 generators, 1538 loads, and 3319 branches.

The Taipower system is the only transmission system in Taiwan. Its transmission lines run from north to south, encompassing a distance of roughly 400 km. The Taipower system is divided into three regions: the northern, central, and southern regions. The regions are interconnected using several 345 kV transmission lines, as shown in Figure 11. Indeed, the majority of the loads are distributed in northern Taiwan, whereas most of the power plants are located in central and southern Taiwan. In this manner, most of the power in Taiwan is sent from the central or southern region to the northern region. This may result in severe imbalances between supply and demand. Thus, voltage collapse has always been a concern in the Taipower system.

A series of simulations with respect to various loading conditions and Q limit violations has been conducted. The results in terms of L_{max} for the test cases listed in Table 1 are shown in Figure 12. From the shown figure, it reveals that the values of L_{max} given by the proposed method are very close to 1. However, the values of L_{max} given by the RM are much less than 1. This means that the presented method can be utilized as an absolute indicator in voltage stability analysis.

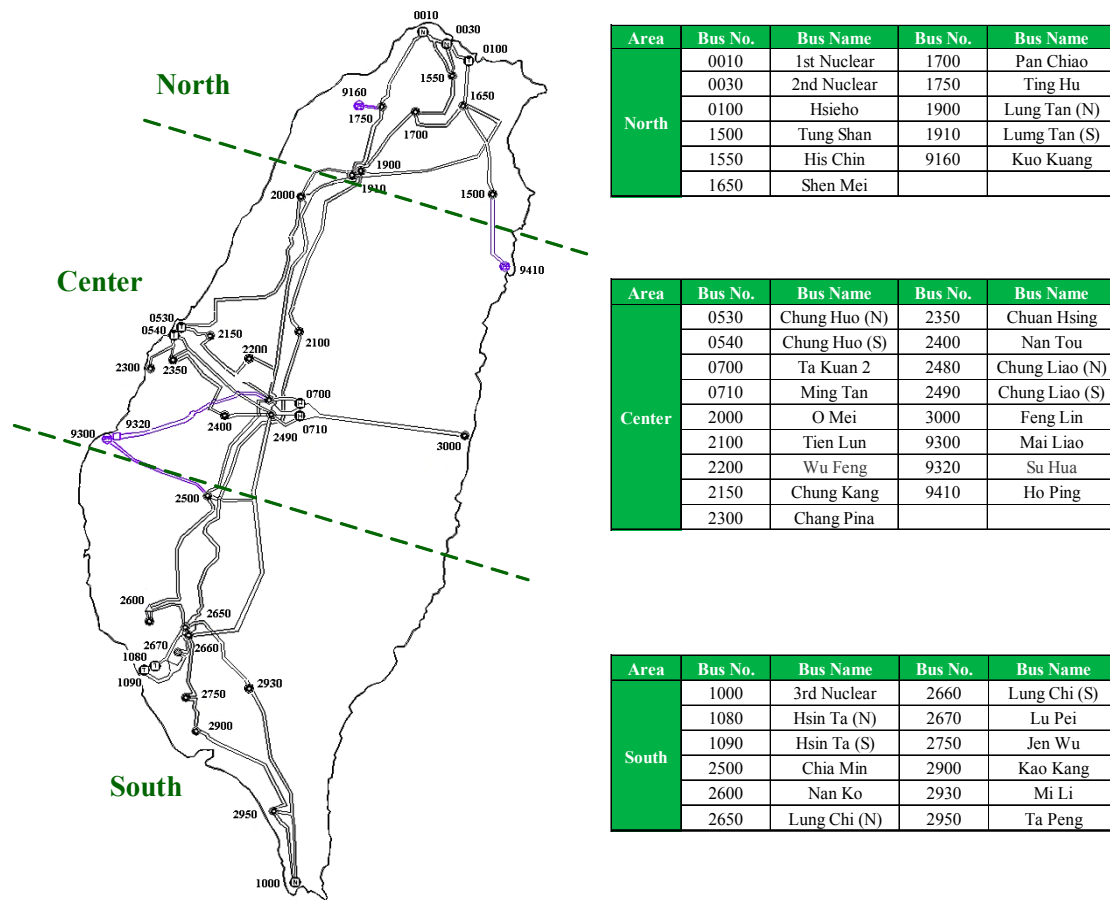


Figure 11. Simplified diagram of Taipower system.

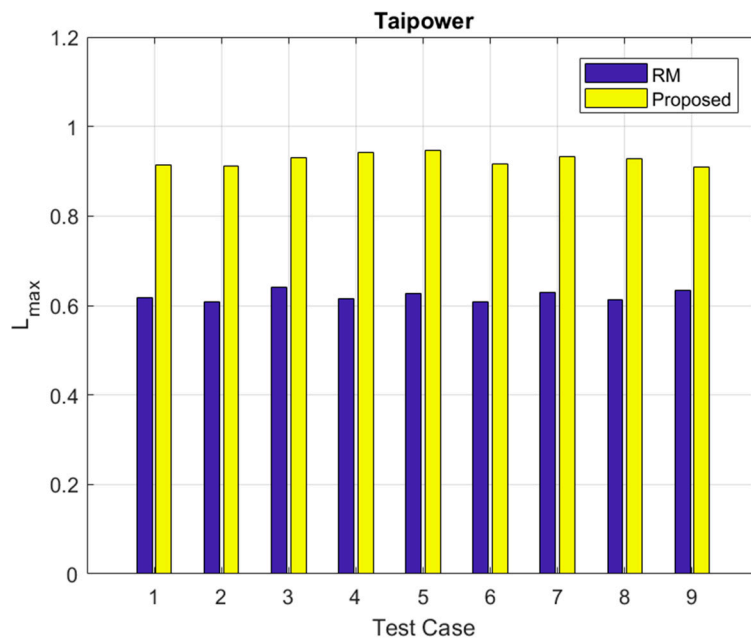


Figure 12. Comparisons for system load at voltage collapse point under different test cases in Taipower system. A higher L_{max} indicates a better performance.

4.4. Consideration of ZIP Load Model

Since voltage stability is affected by load characteristics, the composite ZIP load model, which consists of constant impedance, constant current, and constant power, is considered in this paper as well. The ZIP model is given by

$$\begin{aligned} P &= P_0 \left[a_0 (V/V_0)^2 + a_1 (V/V_0) + a_2 \right] \\ Q &= Q_0 \left[a_0 (V/V_0)^2 + a_1 (V/V_0) + a_2 \right] \end{aligned} \quad (24)$$

where P_0 and Q_0 are the active and reactive power demand at nominal voltage V_0 , respectively; a_0 , a_1 , and a_2 are constants and $a_0 + a_1 + a_2 = 1$. In this work, the composite model with 20% constant impedance, 20% constant current, and 60% constant power are considered. Thus, those three constants are, respectively, set to be $a_0 = 0.2$, $a_1 = 0.2$, and $a_2 = 0.6$.

The IEEE 39-bus system with ZIP load model is utilized as a test example to demonstrate the effectiveness of the presented approach. The considered system comprises of 39 buses, 47 branches, 18 loads, and 10 generators. A lot of simulations have been conducted on this test system. The results based on the cases given in Table 1 are illustrated in Figure 13, showing that the proposed approach is superior over the RM even under the consideration of composite load model.

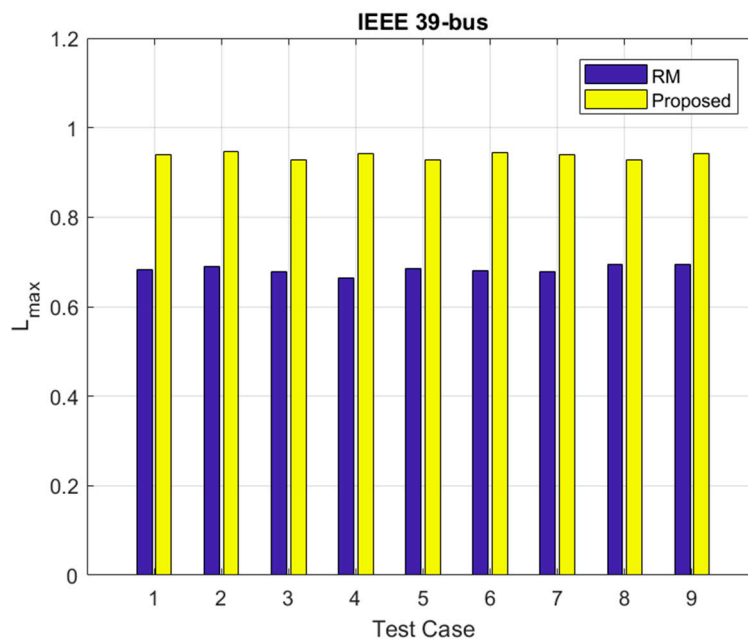


Figure 13. Comparisons for system load at voltage collapse point under different test cases in IEEE 39-bus model. A higher L_{max} indicates a better performance.

5. Conclusions

A novel methodology for on-line voltage stability monitoring was developed in this paper. It is based on the GECM and the WAMS. In the developed methodology, the RLS algorithm with synchrophasor data are first employed to track changing parameters of transmission grid impedance models, when considering the dynamic behavior of system generators. The estimated models are then used in the computation of the enhanced voltage stability index that was capable to provide accurate indicator of transmission grid voltage instability not only under normal conditions but also under generator Q-limit violations. Multiple power grids under various operating conditions are utilized to illustrate the accuracy and capability of the presented methodology.

Acknowledgments: This work was supported by the Ministry of Science and Technology of Taiwan, under Contract MOST 106-2221-E-035-064 and Contract MOST 106-3113-E-002-012.

Author Contributions: Heng-Yi Su proposed the approach and wrote the manuscript with input from Tzu-Yi Liu.

Conflicts of Interest: The authors declare no conflict of interest.

Abbreviations

The following abbreviations are used in this manuscript.

WAMS	Wide-Area Measurement System
GECM	Generator Equivalent Circuit Model
PMU	Phasor Measurement Unit
RLS	Recursive Least Squares
TE	Thevenin Equivalent
GPS	Global Positioning System
RM	Reference Method
KVL	Kirchoff's Voltage Law

References

1. Ajarapu, V. *Computational Techniques for Voltage Stability Assessment and Control*; Springer: New York, NY, USA, 2006.
2. Lim, J.M.; DeMarco, C.L. SVD-based voltage stability assessment from phasor measurement unit data. *IEEE Trans. Power Syst.* **2016**, *31*, 2557–2565. [[CrossRef](#)]
3. Hu, F.; Sun, K.; Del Rosso, A.; Farantatos, E.; Bhatt, N. Measurement-based real-time voltage stability monitoring for load areas. *IEEE Trans. Power Syst.* **2016**, *31*, 2787–2798. [[CrossRef](#)]
4. Andersson, G.; Donalek, P.; Farmer, R.; Hatziaargyriou, N.; Kamwa, I.; Kundur, P.; Martins, N.; Paserba, J.; Pourbeik, P.; Sanchez-Gasca, J.; et al. Causes of the 2003 major grid blackouts in north America and Europe, and recommended means to improve system dynamic performance. *IEEE Trans. Power Syst.* **2005**, *20*, 1922–1928. [[CrossRef](#)]
5. Simpson-Porco, J.W.; Dörfler, F.; Bullo, F. Voltage collapse in complex power grids. *Nat. Commun.* **2016**, *7*, 10790. [[CrossRef](#)] [[PubMed](#)]
6. Phadke, A.G.; Thorp, J.S. *Synchronized Phasor Measurements and Their Applications*; Springer: New York, NY, USA, 2008.
7. Aminifar, F.; Fotuhi-Firuzabad, M.; Safdarian, A.; Davoudi, A.; Shahidehpour, M. Synchrophasor measurement technology in power systems: Panorama and state-of-the-art. *IEEE Access* **2014**, *2*, 1607–1628. [[CrossRef](#)]
8. Manousakis, N.M.; Korres, G.N.; Georgilakis, P.S. Taxonomy of PMU placement methodologies. *IEEE Trans. Power Syst.* **2012**, *2*, 1070–1077. [[CrossRef](#)]
9. Chen, C.; Wang, J.; Li, Z.; Sun, H.; Wang, Z. PMU uncertainty quantification in voltage stability analysis. *IEEE Trans. Power Syst.* **2015**, *30*, 2196–2197. [[CrossRef](#)]
10. Zhao, J.; Wang, Z.; Chen, C.; Zhang, G. Robust voltage instability predictor. *IEEE Trans. Power Syst.* **2017**, *32*, 1578–1579. [[CrossRef](#)]
11. Vournas, C.D.; Lambrou, C.; Mandoulidis, P. Voltage stability monitoring from a transmission bus PMU. *IEEE Trans. Power Syst.* **2017**, *32*, 3266–3274. [[CrossRef](#)]
12. Su, H.-Y.; Liu, T.-Y. A PMU-based method for smart transmission grid voltage security visualization and monitoring. *Energies* **2017**, *10*, 1103.
13. Gao, B.; Morison, G.K.; Kundur, P. Voltage stability evaluation using modal analysis. *IEEE Trans. Power Syst.* **1992**, *7*, 1529–1542. [[CrossRef](#)]
14. Ajarapu, V.; Christy, C. The continuation power flow: A tool for steady state voltage stability analysis. *IEEE Trans. Power Syst.* **1992**, *7*, 416–423. [[CrossRef](#)]
15. Chiang, H.D.; Flueck, A.J.; Shah, K.S.; Balu, N. CPFLOW: A practical tool for tracing power system steady-state stationary behavior due to load and generation variations. *IEEE Trans. Power Syst.* **1995**, *10*, 623–634. [[CrossRef](#)]

16. Sun, T.; Li, Z.; Rong, S.; Lu, J.; Li, W. Effect of Load Change on the Thevenin Equivalent Impedance of Power System. *Energies* **2017**, *10*, 330. [[CrossRef](#)]
17. Vu, K.; Begovic, M.M.; Novosel, D.; Saha, M.M. Use of local measurements to estimate voltage-stability margin. *IEEE Trans. Power Syst.* **1999**, *14*, 1029–1035. [[CrossRef](#)]
18. Smon, I.; Verbic, G.; Gubina, F. Local voltage-stability index using Tellegen's theorem. *IEEE Trans. Power Syst.* **2006**, *21*, 1267–1275. [[CrossRef](#)]
19. Wang, Y.; Pordanjani, I.R.; Li, W.; Xu, W.; Chen, T.; Vaahedi, E.; Gurney, J. Voltage stability monitoring based on the concept of coupled single-port circuit. *IEEE Trans. Power Syst.* **2011**, *4*, 2154–2163. [[CrossRef](#)]
20. Liu, J.H.; Chu, C.C. Wide-area measurement-based voltage stability indicators by modified coupled single-port models. *IEEE Trans. Power Syst.* **2014**, *2*, 756–764. [[CrossRef](#)]
21. Su, H.Y.; Liu, C.W. Estimating the voltage stability margin using PMU measurements. *IEEE Trans. Power Syst.* **2016**, *31*, 3221–3229. [[CrossRef](#)]
22. Cui, B.; Wang, Z. Voltage stability assessment based on improved coupled single-port method. *IET Gener. Transm. Distrib.* **2017**, *11*, 2703–2711. [[CrossRef](#)]
23. Wang, Y.; Wang, C.; Lin, F.; Li, W.; Wang, L.Y.; Zhao, J. Incorporating generator equivalent model into voltage stability analysis. *IEEE Trans. Power Syst.* **2013**, *4*, 4857–4866. [[CrossRef](#)]
24. Kessel, P.; Glavitsch, H. Estimating the voltage stability of a power system. *IEEE Trans. Power Deliv.* **1986**, *3*, 346–354. [[CrossRef](#)]
25. Acharya, N.V.; Rao, P.S.N. A new voltage stability index based on the tangent vector of the power flow jacobian. In Proceedings of the 2013 IEEE Innovative Smart Grid Technologies-Asia (ISGT Asia), Bangalore, India, 10–13 November 2013; pp. 1–6.
26. Kundur, P. *Power System Stability and Control*; McGraw-Hill: New York, NY, USA, 1994.
27. Sauer, P.W.; Pai, M.A. *Power System Dynamics and Stability*; Prentice-Hall: Upper Saddle River, NJ, USA, 1998.
28. Milano, F. *Power System Analysis Toolbox (PSAT)*, version 2.0.0.; University College Dublin: Dublin, Ireland, 2008.
29. Power Systems Test Case Archive, University of Washington College of Engineering. Available online: <http://www.ee.washington.edu/re-serach/pstcal/> (accessed on 14 April 2017).



© 2017 by the authors. Licensee MDPI, Basel, Switzerland. This article is an open access article distributed under the terms and conditions of the Creative Commons Attribution (CC BY) license (<http://creativecommons.org/licenses/by/4.0/>).